Modelling and Simulation of a Transformer With Inter-turn Fault Including Saturation Effect and Variable Fault Parameters

M. Samami*, H. Yaghobi**(C.A.) and M. Niaz Azari***

Abstract: This investigation deals with a mathematical model for a distribution transformer including saturation effect. To this end, the equations related to a three phase transformer are specified and the effect of an inter-turn fault is included. Naturally by applying an inter-turn fault the inductance and resistance matrix will change. Thus, unknown quantities of inductances and resistances for completing the matrix are calculated and the inputs, outputs and state variables are specified. All the equations will be rewritten in terms of state variables, subsequently saturation effect is added to the model. Finally the block diagram of the specified model based on the obtained equations are designed and the ultimate model is simulated. The saturation effect, added to the mathematical model and also the variable fault parameters are known as two significant contributions which distinguish this study from other investigations. Various results obtained from the simulation of the final model confirm the changes in the behavior of faulty transformer such as: a large circulating current flowing in the shorted turns, lower impact on terminal voltages and currents, a sudden increase in current flowing in the primary winding, asymmetrical flux distribution and inverse proportion of the fault severity and the limiting resistor.

Keywords: Inductance, Inter-turn, Modelling, Saturation Effect, Transformer.

1 Introduction

1.1 Transformer Fault Classification

A transformer as a vital part of a power system, plays an important role in the transmission process of generated energy in power plants and distribution of it to a point of power utilization. In today's world, due to the incremental rate of complex loads in power networks with various control systems which causes an amazing network expansion, transformers are seriously and continuously exposed to risks. This fact is the main reason that necessitates the Recognition; classification and urgent detection of transformer faults. Accordingly, the faults can be categorized as external and internal [1]. The external faults involve; overloading, voltage increase due to impulse excitation, short circuit in the network and etc. Whereas, the internal faults involve; winding defects, winding insulation failures, oil decomposition, core faults, defects in the mechanism of tap-changer and etc. Among all the mentioned faults, winding insulation failures are always considered as the most important reason of power transformer outage, which are usually categorized as static and dynamic failures [2], [3]. The reason of static failure is winding insulation defect during manufacturing. But the important factors that cause dynamic failures include; over voltages caused by lightning, over voltages caused by switching, inrush current of transformers, prolonged overloading and failure of the cooling mechanism.

Inter-turn fault is known as a famous reason of insulation failure in transformers. Transient over voltages, caused by impulse excitation, is a determinative factor in creation of winding inter-turn fault. Thus, overvoltage distribution along the winding must be uniform [4]. It should be noted that, urgent detection of inter-turn fault has a great importance in preventing the increment of fault severity [5].

1.2 Literature Review and Contribution

Various methods have been proposed in order to detect inter-turn fault which are completely mentioned in Table 1. On the other hand, the disadvantages of the applied methods are presented in Table 2.

In [22], [23], the behavior of transformers are analyzed with high emphasis on experimental models.

Iranian Journal of Electrical & Electronic Engineering, 2017.
Paper first received 07 Septempber 2016 and in revised form 10 April 2017.
* The author is with Mah Taab Caspian Electricity Generation Company, Nowshahr Power Plant, Nowshahr, Iran.
E-mail: mehdisamami63@gmail.com.
** The author is with the Faculty of Electrical and Computer Engineering, Semnan University, Semnan, Iran.
E-mail: yaghobi@semnan.ac.ir.
*** The author is with the Faculty of Electrical Engineering, University of Science and Technology of Mazandaran, Behshahr, Iran.
E-mail: miladniazazari@mazust.ac.ir.
Corresponding Author: H. Yaghobi.

Table 1 Description of some important methods for internal fault detection.

Methods	Ref.	Remarks and essential descriptions
Differential Protection	[1], [6], [7]	• Differential relays measure the primary and secondary phase current of the transformer and convert them to a mutual base value which is comparable with the calculated differences in the currents.
	[1], [6], [7]	• Small current differences indicates the normal operation of the transformer and also external fault occurrence condition. This small value is equal to the magnetizing and also the core loss of the current. But this difference value becomes greater during an internal fault.
Dissolved Gas Analysis (DGA)	[8], [9]	• Transformer oil and its winding insulation can be destructed and decomposed to different gases due to thermal or electrical stress. A range of generated amount of gases between 0-500 ppm, shows the normal operation of transformer.
	[10], [11]	• The high amount of circulating current caused by an internal fault can be detected with obtained DGA data, applied by various methods such as Rogers Ratio method.
Frequency Response Analysis (FRA)	[12]- [14]	• Due to high dependency of winding admittance to the operating frequency, the FRA is introduced as another method for detection of inter-turn fault. In this method the admittance is measured in a wide range of frequency.
	[15]	• The responses in this method are categorized as low, medium and high frequency response. But only low and high frequency responses are considered to be significant in frequency analysis of inter-turn faults.
	[16], [17]	• This method can also be used in order to detect deformation of windings due to short circuit fault, and also diagnosis of core fault.
Advanced Methods	[18]- [20] [21]	These methods include • Wavelet transform and Artificial neural networks • Fuzzy logic

Table 2 The disadvantages of the mentiond method for internal fault detection.

Methods	Disadvantages
Differential protection	• The differential method has high sensitivity to measurement accuracy of the current transformers. Therefore an algorithm for compensation of measurement through mathematical fault correction, generated by current transformers, is always needed. • Inaccessibility to phase terminals in the transformers with delta connections for measurement of the phase currents
Dissolved gas analysis (DGA) (DGA)	• The results and forecasts derived from dissolved gas analysis method such as local overheating and high circulating current can also be created by other internal faults in addition to inter-turn fault. Therefore, this method can cause ambiguity in determining the precise type of fault. • This method is not suitable for dry transformers, transformers with a natural cooling mechanism and transformers with air forced cooling mechanism.
frequency response analysis (FRA)	• FRA always requires additional equipment for diagnosis. • The prediction of operating conditions is not easily possible due to complex admittances, and always requires an expert's opinion and evidential reasons.
Advanced methods	• These methods are not practical. As an example, in artificial neural networks the neural current is not easily available for transformers. Besides, advanced calculation methods always require a large number of powerful processors.

But considering the high price of transformers and difficult accessibility to the equipment required for performing the experiment, this method is not feasible for everyone. Furthermore, analyzing inter-turn fault effects, on accessibility to the equipment required for performing the experiment, this method is not feasible for everyone. Furthermore, analyzing inter-turn fault effects, on transformers with different characteristics and in different voltage levels requires multiple experimental models which is illogical from economic point of view. In [24], a model based on flux rearrangement around the damaged turns has been developed. But the mentioned model is very simple and only simulated a single phase transformer. On the other hand, it does not have transformative fault parameters including changeable fault resistance and also changeable number of faulty turns of transformer winding. Ref. [22], [25], [26], present a finite element model (FEM) of a transformer in addition to an experimental model. The various aforementioned models of the transformer, with inter-turn fault, are based on finite element analysis, mathematical model without consideration of saturation effect and also limited experimental models in accordance to the specifications of the transformer which are given in the transformer plaque. In fact, none of the published papers have presented a flexible model, based on mathematical equation, considering linkage and leakage flux of the transformer (changeable self and mutual inductances). On the other hand, the aforementioned models do not

have flexibility for different fault severity. Therefore, providing a transformer approximate model including inter-turn fault which can operate under

- ✓ different nominal specification of the transformer
- ✓ different winding resistance and inductances (changeable resistance and also self and mutual inductances)
- ✓ various fault resistance and fault severity (the ability to present an acceptable flux analysis)
- ✓ various involved number of turns in the faulty winding
- ✓ selective fault in each section of each winding
- ✓ consideration of the core saturation effect

seems to be essential.

The mentioned model is proposed to achieve a better understanding from the behavior of distribution transformers with inter-turn fault in a frame of a flexible model based on mathematical equations, with the ability to change the fault parameters including fault severity and the number of shorted turns of the primary winding. Different parameters of transformer such as voltage, frequency, inductance, resistance and etc are changeable. It should be noted that, the saturation effect is included in the model as well. This paper is based on mathematical equations of a transformer with inter-turn fault. Therefore, the passive parameters, caused by inter-turn fault, should be specified. Then, the equations are rewritten according to new status, considering the saturation effect. Finally the obtained block diagram of the specified model is designed and simulated.

2 Three-Phase Transformer Model, with Inter-turn Fault

A sample model for a normal 3-phase transformer is well known [27]. The resistance and inductance matrix for a normal operated 3-phase transformer are also presented in [27]. Imposing an inter-turn fault to phase 'B' of the transformer primary winding divides the mentioned coil into two segments including sub-coils 'a', and 'sh', as shown in Fig. 1, [27].

$$r=\begin{bmatrix} r_1 & 0 & 0 & 0 & 0 & 0 & 0 \\ 0 & r_2 & 0 & 0 & 0 & 0 & 0 \\ 0 & 0 & r_a & 0 & 0 & 0 & 0 \\ 0 & 0 & 0 & r_{sh} & 0 & 0 & 0 \\ 0 & 0 & 0 & 0 & r_4 & 0 & 0 \\ 0 & 0 & 0 & 0 & 0 & r_5 & 0 \\ 0 & 0 & 0 & 0 & 0 & 0 & r_6 \end{bmatrix} \quad (1)$$

$$L=\begin{bmatrix} L_{11} & L_{12} & L_{1a} & L_{1sh} & L_{14} & L_{15} & L_{16} \\ L_{21} & L_{22} & L_{2a} & L_{2sh} & L_{24} & L_{25} & L_{26} \\ L_{a1} & L_{a2} & L_{aa} & L_{ash} & L_{a4} & L_{a5} & L_{a6} \\ L_{sh1} & L_{sh2} & L_{sha} & L_{shsh} & L_{sh4} & L_{sh5} & L_{sh6} \\ L_{41} & L_{42} & L_{4a} & L_{4sh} & L_{44} & L_{45} & L_{46} \\ L_{51} & L_{52} & L_{5a} & L_{5sh} & L_{54} & L_{55} & L_{56} \\ L_{61} & L_{62} & L_{6a} & L_{6sh} & L_{64} & L_{65} & L_{66} \end{bmatrix}$$

As a result, the resistance and inductance matrix will change to, 7*7 matrix with unknown parameters as shown in (1). It should be stated that, the quantities of the faulty sub-coil, are shown with, '*sh*' index and the red colored parameters are known as passive parameters which should be calculated subsequently.

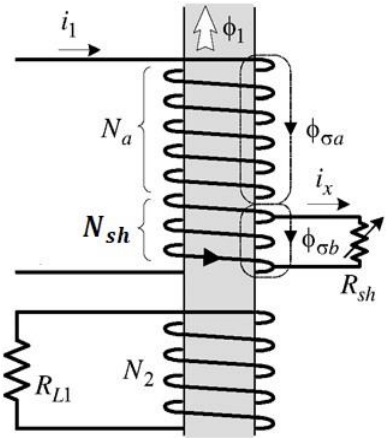

Fig. 1 Inter-turn fault modelling in a distribution transformer [28].

2.1 Determination of inductances and resistances

Passive resistance quantities depend on the ratio between, the number of turns in each sub-coil to the general number of turns in the faulty (primary) winding [27]. The unknown quantities of inductance matrix are specified by three important rules including: consistency, proportionality and leakage [27]. It is necessary to mention that, leakage factors, such as σ_{ash}, σ_{shi} and σ_{ai}, are considered as known parameters. In fact, leakage factors have a strong relationship with the geometry of transformers and it is the main reason which makes these factors hard to obtain. However, the leakage factors can be approximated by neglecting the leakage flux outside the windings and assuming it to flow completely parallel to the axis of transformer windings [29].

Each winding inductance consists of, self and mutual inductance. For instance:

$$\begin{aligned} L_{aa} &= \left(L_{La}+L_{ma}\right) \\ L_{33} &= \left(L_{L3}+L_{m3}\right) \\ L_{shsh} &= \left(L_{Lsh}+L_{msh}\right) \end{aligned} \quad (2)$$

In accordance to the mentioned rules, the unknown self and mutual inductances of the inductance matrix are calculated by a numerical resolution method, as follows:

$$L_{aa}=L_{33}*\left(\frac{n_a}{n_3}\right)^2 \quad (3)$$

Consequently, L_{shsh} can be obtained by replacing n_{sh}

instead of n_a in (3).

$$L_{ash} = L_{sha} = L_{33} * \left(\frac{n_a}{n_3}\right)\left(\frac{n_{sh}}{n_3}\right)$$

$$= \frac{n_{sh}}{n_a} L_{aa} = \frac{n_{sh}}{n_a}\left(L_{La} + L_{ma}\right) \quad (4)$$

But other inductances including, mutual inductances among the sub-coils of faulty winding in phase 'B', and other windings are still unknown, which are calculated by assuming:

$$\frac{L_{ai}}{L_{shi}} = \frac{n_a}{n_{sh}} = k \quad (5)$$

Thus, the mentioned inductances are given by:

$$L_{ai} = L_{ia} = \frac{k}{1+k} = \frac{\frac{n_a}{n_{sh}}}{1+\frac{n_a}{n_{sh}}} = \frac{\frac{n_a}{n_{sh}}}{\frac{n_{sh}+n_a}{n_{sh}}} = \frac{n_a}{n_3} L_{3i} \quad (6)$$

$$L_{shi} = L_{ish} = \frac{1}{1+k} = \frac{1}{1+\frac{n_a}{n_{sh}}} = \frac{n_{sh}}{n_3} L_{3i} \quad (7)$$

However, by assuming a typical winding to be wound on the same leg as the sub-coils of faulty (phase 'B' of primary) winding, the equations will be different for that. In this method the sub-coil of the faulty winding which has the largest number of turns will be selected. Suppose, sub-coils 'a' has the largest number of turns between two sub-coils. As a result, the following equation is specified.

$$\frac{\sigma_{ai}}{\sigma_{3i}} = \varepsilon \quad (8)$$

As mentioned before, different leakage factors such as σ_{ai}, σ_{shi} and σ_{3i} are assumed to be known. Thus, for obtaining the unknown inductances, the following formula is obtained.

$$L_{ai} = L_{ia} = L_{3i}\sqrt{\varepsilon}\sqrt{\frac{L_{aa}}{L_{33}}}\sqrt{1+\frac{1-\varepsilon}{\varepsilon}\frac{L_{33}L_i}{L_{3i}^{\ 2}}} \quad (9)$$

And as a result of consistency principle L_{shi} can be calculated as follows.

$$L_{shi} = L_{3i} - L_{ai} \quad (10)$$

2.2 Voltage Equations

The faulty phase voltage equations of the primary winding, considering an inter-turn fault occurred on phase 'B', with certain number of turns which is shown by n_{sh}, can be written as

$$v_3 = r_a i_a + z_f\left(i_a + i_{circulating}\right) + p\lambda_a \quad (11)$$

$$v_{sh} = r_{sh} i_{sh} + p\lambda_{sh} \quad (12)$$

where z_f is the fault impedance, $i_{circulating}$ is the circulating current caused by inter-turn fault in the shorted turns, v_{sh} and r_{sh} represent the voltage and the resistance of the shorted turns, respectively, and $p = d/dt$. The voltage equations for healthy windings in both primary and secondary sides in phase 'A' can be written as follows.

$$v_1 = r_1 i_1 + p\lambda_1 \quad (13)$$

$$v_2 = r_2 i_2 + p\lambda_2 \quad (14)$$

Equations of healthy windings in phase 'B' and 'C' can be written in the same way as above. By taking a look at the voltage equations, the induced voltage terms including, $p\lambda_a$, $p\lambda_{sh}$, $p\lambda_1$ and $p\lambda_2$ can be seen obviously. All the induced voltage terms depend on inductances. Besides, after the occurrence of an inter-turn fault the inductance matrix will change, which involves known and unknown arrays. Thus, for completing the voltage equations in details, the unknown quantities should be rewritten based on the known inductances and considering three important rules including consistency, leakage and proportionality, as mentioned before.

2.3 Determination of the Induced Voltage Equations

By assuming

$$n_1 = n_3 = n_5$$
$$n_2 = n_4 = n_6 \quad (15)$$

The first induced voltage term of faulty winding is $p\lambda_a$ which can be written, based on L_{L3} and L_{m3}. For this purpose, the flux equation should be written based on the flux matrix as follows:

$$\lambda_a = L_{a1} i_1 + L_{a2} i_2 + L_{aa} i_a + L_{ash} i_{sh} + L_{a4} i_4 + L_{a5} i_5 + L_{a6} i_6 \quad (16)$$

In the next step, the unknown inductances will be replaced in accordance to (3)-(10), as expressed below.

$$\lambda_a = L_{L3}\left(\left(\frac{n_a}{n_3}\right)^2 i_a + \frac{n_a}{n_3}\frac{n_{sh}}{n_3} i_{sh}\right) + L_{m3}\left(\frac{n_a}{n_3} i_1 + \frac{n_a}{n_3} i_2 + \left(\frac{n_a}{n_3}\right)^2 i_a + \frac{n_a}{n_3}\frac{n_{sh}}{n_3} i_{sh} + \frac{n_a}{n_3} i_4 + \frac{n_a}{n_3} i_5 + \frac{n_a}{n_3} i_6\right) \quad (17)$$

Finally, derivative of (17), represents the induced voltage of sub-coil 'a', and will be written as

$$e_a = p\lambda_a = L_{L3}\left(\left(\frac{n_a}{n_3}\right)^2 \frac{di_a}{dt} + \frac{n_a}{n_3}\frac{n_{sh}}{n_3}\frac{di_{sh}}{dt}\right)$$
$$+L_{m3}\left(\begin{array}{l}\frac{n_a}{n_3}\frac{di_1}{dt} + \frac{n_a}{n_3}\frac{d\,i_2}{dt} + \left(\frac{n_a}{n_3}\right)^2 \frac{di_a}{dt} + \frac{n_a}{n_3}\frac{n_{sh}}{n_3}\frac{di_{sh}}{dt} \\ + \frac{n_a}{n_3}\frac{d\,i_4}{dt} + \frac{n_a}{n_3}\frac{di_5}{dt} + \frac{n_a}{n_3}\frac{d\,i_6}{dt}\end{array}\right) \quad (18)$$

The second induced voltage term of the faulty winding is, $p\lambda_{sh}$ which can be calculated in the same way as $p\lambda_a$. The final equation will be as follows

$$e_{sh} = p\lambda_{sh} = L_{L3}\left(\left(\frac{n_{sh}}{n_3}\right)^2 \frac{di_{sh}}{dt} + \frac{n_{sh}}{n_3}\frac{n_a}{n_3}\frac{di_a}{dt}\right)$$
$$+L_{m3}\left(\begin{array}{l}\frac{n_{sh}}{n_3}\frac{di_1}{dt} + \frac{n_{sh}}{n_3}\frac{d\,i_2}{dt} + \left(\frac{n_{sh}}{n_3}\right)^2 \frac{di_{sh}}{dt} + \frac{n_{sh}}{n_3}\frac{n_a}{n_3}\frac{di_a}{dt} \\ + \frac{n_{sh}}{n_3}\frac{d\,i_4}{dt} + \frac{n_{sh}}{n_3}\frac{di_5}{dt} + \frac{n_{sh}}{n_3}\frac{d\,i_6}{dt}\end{array}\right) \quad (19)$$

The induced voltage of phase 'A' and 'C', in the primary winding can be obtained with the same process, as mentioned for the sub-coils of the faulty winding. The induced voltage of phase 'A' is calculated from flux equation as follows.

$$\lambda_1 = L_{11}i_1 + L_{12}i_2 + L_{1a}i_a + L_{1sh}i_{sh} + L_{14}i_4 + L_{15}i_5 + L_{16}i_6 \quad (20)$$

The following equations are obtained, According to Ref. [29].

$$L_{1i} = \frac{n_i}{n_1}L_{m1} \quad (21)$$

$$\frac{L_{m1}}{L_{m2}} = \left(\frac{n_1}{n_2}\right)^2 \quad (22)$$

With the help of (2) and (21), the flux equation becomes

$$\lambda_1 = L_{L1}i_1 + L_{m1}\left(\begin{array}{l} i_1 + i_2 + \frac{n_a}{n_1}i_a + \frac{n_{sh}}{n_1}i_{sh} \\ + i_4 + i_5 + i_6\end{array}\right) \quad (23)$$

The derivative of (23), represents the induced voltage of phase 'A' in primary winding as follows:

$$e_1 = p\lambda_1 = L_{L1}\frac{di_1}{dt} + L_{m1}\left(\begin{array}{l}\frac{di_1}{dt} + \frac{d\,i_2}{dt} + \frac{n_a}{n_1}\frac{di_a}{dt} + \frac{n_{sh}}{n_1}\frac{di_{sh}}{dt} \\ + \frac{d\,i_4}{dt} + \frac{di_5}{dt} + \frac{d\,i_6}{dt}\end{array}\right) \quad (24)$$

Considering, $L_{m1} = L_{m3} = L_{m5}$ and also $L_{m2} = L_{m4} = L_{m6}$, The ultimate induced voltage equation of phase 'C', can be written with the same process, as phase 'A'. For completing (14) which is known as the secondary voltage equation of phase 'A', the secondary induced voltage including, $p\lambda_2$, should be calculated. The induced voltage of the mentioned phase in secondary side is calculated from the flux equation as

$$\lambda_2 = L_{21}i_1 + L_{22}i_2 + L_{2a}i_a + L_{2sh}i_{sh} + L_{24}i_4 + L_{25}i_5 + L_{26}i_6 \quad (25)$$

The unknown parameters of (25) is calculated in accordance to (3)-(10), as previously mentioned and the equation becomes

$$\lambda_2 = L_{L2}i_2 + L_{m2}\left(\begin{array}{l}\frac{n_1}{n_2}i_1 + i_2 + \frac{n_a}{n_2}i_a + \frac{n_{sh}}{n_2}i_{sh} \\ + \frac{n_4}{n_2}i_4 + \frac{n_5}{n_2}i_5 + \frac{n_6}{n_2}i_6\end{array}\right) \quad (26)$$

With the help of the equations which are used for referring the quantities of winding secondary side, to winding primary side [29], and by multiplying both sides of (26) by (n_2/n_1), the following equation is obtained.

$$\frac{n_2}{n_1}\lambda_2 = L_{L2}\,i_2 + L_{m1}\left(\frac{n_2}{n_1}\right)^2\left(\begin{array}{l} i_1 + i_2 + i_4 + i_5 + i_6 \\ + \frac{n_a}{n_2}\frac{n_2}{n_1}i_a + \frac{n_{sh}}{n_2}\frac{n_2}{n_1}i_{sh}\end{array}\right) \quad (27)$$

By dividing both sides of (27) to $(n_2/n_1)^2$, the final flux equation can be written as

$$\lambda_2 = L_{L2}\,i_2 + L_{m1}\left(\begin{array}{l} i_1 + i_2 + \frac{n_a}{n_1}i_a + \frac{n_{sh}}{n_1}i_{sh} \\ + i_4 + i_5 + i_6\end{array}\right) \quad (28)$$

The derivative of (28), represents the induced voltage of phase 'A', in secondary winding as follows:

$$e_2 = L_{L2}\frac{d\,i_2}{dt} + L_{m1}\left(\begin{array}{l}\frac{di_1}{dt} + \frac{d\,i_2}{dt} + \frac{n_a}{n_1}\frac{di_a}{dt} + \frac{n_{sh}}{n_1}\frac{di_{sh}}{dt} \\ + \frac{d\,i_4}{dt} + \frac{di_5}{dt} + \frac{d\,i_6}{dt}\end{array}\right) \quad (29)$$

The induced voltages of phase 'B' and 'C' in secondary winding side, are obtained the same as phase 'A' and in accordance to (25)-(29). It is worth noting that, the first term of all induced voltage equations shows the leakage inductance, and the second term of the mentioned equations presents the core model.

2.4 Simulation of Three-Phase Transformer

As mentioned earlier, for simulation of 3- phase transformer with inter-turn fault, specification of input, output and state variables are needed. In this simulation voltages are considered as input, currents are considered as output and the total flux is used as state variable. The total flux linkages of windings are known as state variables. Thus we have 7 state variables. In terms of these 7 state variables, the voltage equation of the faulty winding can be rewritten as follows:

$$v_3 = r_a i_a + z_f \left(i_a + i_{circulating}\right) + \frac{1}{\omega_b}\frac{d\psi_a}{dt} \quad (30)$$

$$v_{sh} = r_{sh} i_{sh} + \frac{1}{\omega_b}\frac{d\psi_{sh}}{dt} \quad (31)$$

It is noteworthy that, other voltage equations can be rewritten in the same way. As previously mentioned, (17) represents the related flux of sub-coil 'a' in the faulty winding in primary. By rewriting (17), based on ψ, the following relation is obtained.

$$\psi_a = x_{L3}\left(\left(\frac{n_a}{n_3}\right)^2 i_a + \frac{n_a}{n_3}\frac{n_{sh}}{n_3} i_{sh}\right) + x_{m3}\left(\begin{array}{l} \frac{n_a}{n_3} i_1 + \frac{n_a}{n_3} i_2' + \left(\frac{n_a}{n_3}\right)^2 i_a + \frac{n_a}{n_3}\frac{n_{sh}}{n_3} i_{sh} \\ + \frac{n_a}{n_3} i_4' + \frac{n_a}{n_3} i_5 + \frac{n_a}{n_3} i_6' \end{array}\right) \quad (32)$$

where $\psi_a = \omega_b \lambda_a$, and ω_b is the base frequency which is used for reactance calculation. It is noteworthy that, ψ_{sh} is also obtained in the same way. By rewriting (23) and (28) for two other windings, both in primary and secondary sides in a similar way, based on ψ, the following formulas are obtained.

$$\psi_1 = x_{L1} i_1 + x_{m1}\left(\begin{array}{l} i_1 + i_2' + \frac{n_a}{n_1} i_a + \frac{n_{sh}}{n_1} i_{sh} + i_4' \\ + i_5 + i_6' \end{array}\right) \quad (33)$$

$$\psi_2' = x_{L2} i_2' + x_{m1}\left(\begin{array}{l} i_1 + i_2' + \frac{n_a}{n_1} i_a + \frac{n_{sh}}{n_1} i_{sh} + i_4' \\ + i_5 + i_6' \end{array}\right) \quad (34)$$

The final rewritten equations for other phases, both in primary and secondary can be obtained the same as (33) and (34). The second term of (33) and (34), is related to the magnetizing inductance of healthy windings. It can be expressed as

$$\psi_m = x_{m1}\left(i_1 + i_2' + \frac{n_a}{n_1} i_a + \frac{n_{sh}}{n_1} i_{sh} + i_4' + i_5 + i_6'\right) \quad (35)$$

Equation (36) and (37) are related to the magnetizing inductance of sub-coils 'a' and 'sh' in primary, respectively. They can be written as

$$\psi_{m\_a} = \left(\frac{n_a}{n_3}\right) x_{m1}\left(\begin{array}{l} i_1 + i_2' + \frac{n_a}{n_1} i_a + \frac{n_{sh}}{n_1} i_{sh} + i_4' \\ + i_5 + i_6' \end{array}\right) \quad (36)$$

$$\psi_{m\_sh} = \left(\frac{n_{sh}}{n_3}\right) x_{m1}\left(\begin{array}{l} i_1 + i_2' + \frac{n_a}{n_1} i_a + \frac{n_{sh}}{n_1} i_{sh} + i_4' \\ + i_5 + i_6' \end{array}\right) \quad (37)$$

The minimum shorted turns in the faulty winding will cause the highest circulating current. Since, in such situation, n_a is usually close to n_3, it is assumed that, $\psi_m = \psi_{m\_a}$. Thus, we can use (35) instead of (36). The ratio between the linkage flux, passes through the core inside the shorted turns and the same flux passes through the middle of the transformer core inside the healthy turns can be written as follows.

$$\frac{\psi_{m\_sh}}{\psi_m} = \left(\frac{n_{sh}}{n_3}\right) \quad (38)$$

According to (37) and (38) and by assuming a constant supply voltage, occurrence of an inter-turn fault causes decrement of the flux density, flowing through the core, inside the faulty turns. On the other hand, this issue leads to an enhancement of flux density outside the faulty area. The main reason of this phenomenon is the high leakage flux, surrounding the shorted turns unlike the lower amount of flux inside them. In this situation, due to constant supply voltage the fundamental linkage flux does not vary, but a major amount of that, passes the same as leakage flux in a radial form, around the shorted turns and naturally, the leakage flux around these turns becomes stronger, exactly unlike the flux flowing through the core inside the faulty turns [22]. So, by considering (35) and (37) and in accordance to the flux equations, which were previously rewritten, the compact flux equations in the faulty winding and also healthy windings of a sample phase, both in primary and secondary side can be written as

$$\psi_a = x_{L3}\left(\left(\frac{n_a}{n_3}\right)^2 i_a + \frac{n_a}{n_3}\frac{n_{sh}}{n_3} i_{sh}\right) + \psi_m \quad (39)$$

$$\psi_{sh} = x_{L3}\left(\left(\frac{n_{sh}}{n_3}\right)^2 i_{sh} + \frac{n_{sh}}{n_3}\frac{n_a}{n_3} i_a\right) + \psi_{m\_sh} \quad (40)$$

$$\psi_1 = x_{L1} i_1 + \psi_m \quad (41)$$

$$\psi_2' = x_{L2} i_2' + \psi_m \quad (42)$$

The flux equations of other healthy windings are the same as (41) and (42). Thus the currents which are known as outputs of our simulation can be calculated with the help of (39)-(42), and ultimately by substituting the obtained current equations into (35) and by assuming $\frac{n_a}{n_3} = \zeta$, (35) becomes

$$\psi_m = x_{m1}\left(\begin{array}{l} \frac{\psi_1 - \psi_m}{x_{L1}} + \frac{\psi_2' - \psi_m}{x_{L2}'} + \frac{\psi_a - \psi_m}{\zeta x_{L3}} \\ + \frac{\psi_4' - \psi_m}{x_{L4}'} + \frac{\psi_5 - \psi_m}{x_{L5}} + \frac{\psi_6' - \psi_m}{x_{L6}'} \end{array}\right) \quad (43)$$

Equation (43) can be written more compactly as

$$\psi_m = x_M \left(\frac{\psi_1}{x_{L1}} + \frac{\psi_2'}{x_{L2}'} + \frac{\psi_a}{\zeta x_{L3}} + \frac{\psi_4'}{x_{L4}'} + \frac{\psi_5}{x_{L5}} + \frac{\psi_6'}{x_{L6}'} \right)$$
$$\frac{1}{x_M} = \frac{1}{x_{m1}} + \frac{1}{x_{L1}} + \frac{1}{x_{L2}'} + \frac{1}{\zeta x_{L3}} + \frac{1}{x_{L4}'} + \frac{1}{x_{L5}} + \frac{1}{x_{L6}'} \quad (44)$$

Basically, there are different methods for adding saturation to the mentioned simulated model of the 3-phase transformer including inter-turn fault. In this paper, a relation between the saturated and the linear linkage flux is presented according to (45) and Fig. 2. The mentioned figure consists of three regions. The first region is the linear region ($\psi_m^{sat} < B_1$). The second region is called, knee region ($B_1 < \psi_m^{sat} < B_2$). And the third region is the fully saturated region ($\psi_m^{sat} > B_2$) which is approximately linear [29].

$$\psi_m^{unsat} = \psi_m^{sat} + \Delta\psi_m \quad (45)$$

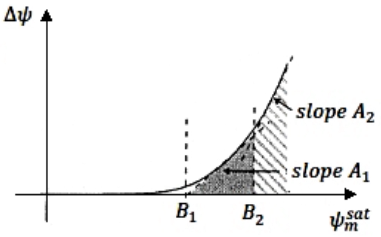

Fig. 2 Piece-wise approximations of $\Delta\psi$ vs. ψ_m^{sat} [29].

In fact, after modelling the saturation effect, ψ_m^{sat} will be used instead of ψ_m^{unsat} in all relations. Therefore, (44) will change as follows

$$\psi_m^{sat} = x_M \left(\frac{\psi_1}{x_{L1}} + \frac{\psi_2'}{x_{L2}'} + \frac{\psi_a}{\zeta x_{L3}} + \frac{\psi_4'}{x_{L4}'} + \frac{\psi_5}{x_{L5}} + \frac{\psi_6'}{x_{L6}'} - \frac{\Delta\psi}{x_m^{unsat}} \right)$$
$$\frac{1}{x_M} = \frac{1}{x_{m1}^{unsat}} + \frac{1}{x_{L1}} + \frac{1}{x_{L2}'} + \frac{1}{\zeta x_{L3}} + \frac{1}{x_{L4}'} + \frac{1}{x_{L5}} + \frac{1}{x_{L6}'} \quad (46)$$

By comparing (44) with (46), it is observed that, the only difference between the linear and saturated model is summarized in an extra term in (46), which is shown by $-\frac{\Delta\psi}{x_m^{unsat}}$ In fact, the saturated model consists of the linear model plus saturation block. The saturation block has a data table with two columns, including $\Delta\psi_m$ values which are written in terms of ψ_m.

With a glance to Equations (44) and (46), it can be concluded that, the saturation block has decreasing effect on the linkage flux, due to the subtractive effect of the extra term, showing by $\frac{\Delta\psi}{x_m^{unsat}}$. In fact the relation between the saturation effect and linkage flux is expressed in Equation (46).

Therefore, any issue which affects the linkage flux can be determinative in core saturation and vice versa.

On the other hand, as previously mentioned, by assuming a constant supply voltage, occurrence of an inter-turn fault causes decrement of the flux density, flowing through the core (linkage flux) extremely unlike the leakage flux. As a result, the linkage flux gets weaker due to an inter turn fault as depicted in the following figure.

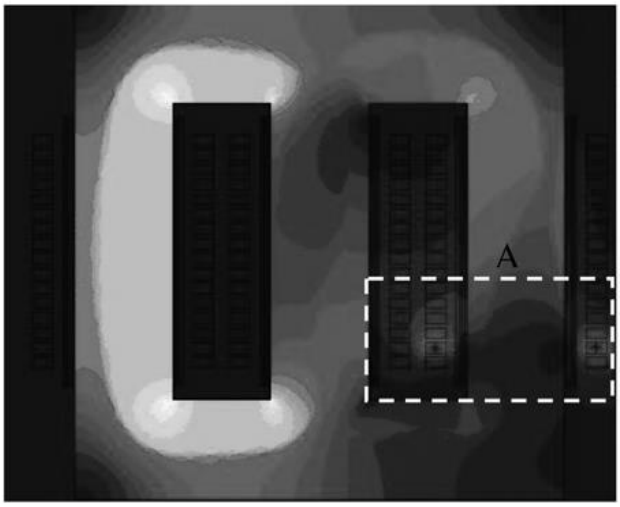

Fig. 3 Flux density distribution inside the transformer under faulty operating condition [22].

Thus, both the saturation effect and inter turn fault have decreasing effect on linkage flux. As a result, occurrence of an inter turn fault under saturation condition leads to sequential decrement of the linkage flux.

By adding the saturation effect, the current equations can be rewritten as presented in (47)-(53).

By substituting the obtained current equations into flux equations the final flux equations are obtained in accordance to (54)-(60).

The saturation effect can also be modeled by three single-phase saturable transformers connected to the primary side of the linear transformer model. In accordance to the mentioned equations, the block diagram of a 3-phase transformer with inter-turn fault, including saturation effect and transformative fault parameters is designed, as shown in Fig. 4.

$$i_1 = \frac{\psi_1 - \psi_m^{sat}}{x_{L1}} \quad (47)$$

$$i_2' = \frac{\psi_2' - \psi_m^{sat}}{x_{L2}'} \quad (48)$$

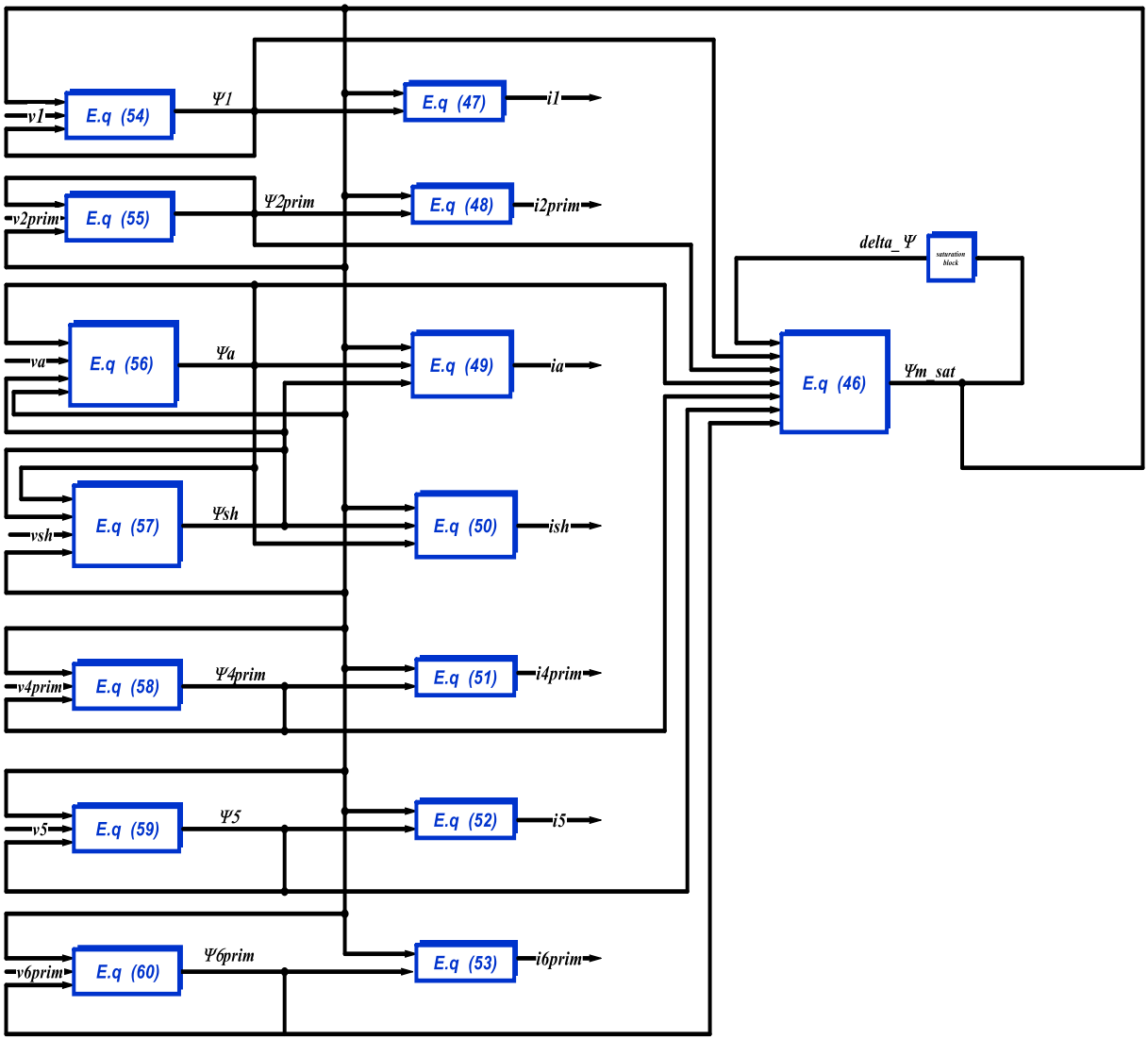

Fig. 4 The block diagram of 3-phase transformer with inter-turn fault including saturation effect.

$$i_a = \left(\frac{n_3}{n_a}\right)^2 \frac{\psi_a - \psi_m^{sat}}{x_{L3}} - \frac{n_{sh}}{n_a} i_{sh} \quad (49)$$

$$i_{sh} = \left(\frac{n_3}{n_{sh}}\right)^2 \frac{\psi_{sh} - \psi_{m-sh}^{sat}}{x_{L3}} - \frac{n_a}{n_{sh}} i_a \quad (50)$$

$$i_4' = \frac{\psi_4' - \psi_m^{sat}}{x_{L4}'} \quad (51)$$

$$i_5 = \frac{\psi_5 - \psi_m^{sat}}{x_{L5}} \quad (52)$$

$$i_6' = \frac{\psi_6' - \psi_m^{sat}}{x_{L6}'} \quad (53)$$

$$\psi_1 = \omega_b \int \left(v_1 - r_1 \left(\frac{\psi_1 - \psi_m^{sat}}{x_{L1}} \right) \right) dt \quad (54)$$

$$\psi_2' = \omega_b \int \left(v_2' - r_2' \left(\frac{\psi_2' - \psi_m^{sat}}{x_{L2}'} \right) \right) dt \quad (55)$$

$$\psi_a = \omega_b \int \left(v_a - r_a \left(\left(\frac{n_3}{n_a}\right)^2 \frac{\psi_a - \psi_m^{sat}}{x_{L3}} - \frac{n_{sh}}{n_a} i_{sh} \right) \right) dt \quad (56)$$

$$\psi_{sh} = \omega_b \int \left(v_{sh} - r_{sh} \left(\left(\frac{n_3}{n_{sh}}\right)^2 \frac{\psi_{sh} - \psi_{m-sh}^{sat}}{x_{L3}} - \frac{n_a}{n_{sh}} i_a \right) \right) dt \quad (57)$$

$$\psi_4' = \omega_b \int \left(v_4' - r_4' \left(\frac{\psi_4' - \psi_m^{sat}}{x_{L4}'} \right) \right) dt \quad (58)$$

$$\psi_5 = \omega_b \int \left(v_5 - r_5 \left(\frac{\psi_5 - \psi_m^{sat}}{x_{L5}} \right) \right) dt \quad (59)$$

$$\psi_6' = \omega_b \int \left(v_6' - r_6' \left(\frac{\psi_6' - \psi_m^{sat}}{x_{L6}'} \right) \right) dt \quad (60)$$

3 Simulation Results and Discussion

The model developed, has been simulated and the following simulation results refer to a 3-phase star-star transformer with an inter-turn fault, imposing to phase 'B' of the transformer primary winding whose characteristics are given as follows:

Table 3 Three-phase transformer parameters

Rated KVA	630
Frequency	50 Hz
Number of turns per phase in primary	360
Number of turns per phase in secondary	120
Primary voltage	4000 v
Secondary voltage	1300 v
Primary resistance	8.25 Ω
Secondary resistance	4.0134 Ω
Primary inductance	0.66 H
Secondary inductance	0.073 H
Mutual inductance	708 H

The result are analyzed by considering different shorted turns (N_{sh}) and various fault resistances (R_f) and with constant load and supplying voltage. Fig. 5 shows different result caused by imposing an inter-turn fault to phase 'B' on primary winding in a three phase transformer, by assuming $N_{sh}=50$ and $R_f=0$.

Occurring an inter-turn fault, whether in primary or secondary, causes a severe voltage drop which leads to a large amount of circulating current flowing in faulty turns. The mentioned circulating current which is shown in Fig. 5(b), arises from the high ratio between the complete winding and the shorted portion of that. It is worth mentioning that, the circulating current is aimed at producing an opposite MMF compared the fundamental MMF of the winding in order to limit the entering flux into the turns. All the above explanations can be justified by Faraday's law.

When an inter-turn fault occurs, whether on the primary or the secondary, a large amount of current flows in the primary winding. The reason for this incremental behavior in the primary winding is, presence of fewer turns for producing the magneto-motive force (MMF) in order to maintain the basic flux of the transformer winding. As previously mentioned, the circulating current flowing in the shorted turns will act as an opposite MMF. On the other hand, the circulating current caused by the inter-turn fault has a large amount and the MMF which is produced by that might be greater than the fundamental MMF. Thus, the inter-turn fault has a significant effect on decrement of fundamental MMF. So inevitably, for having a better MMF compensation, the primary current should be increased. The mentioned behavior is shown in Fig. 5(a).

By dividing the faulty winding to shorted and not shorted turns, the flux waveform of both segments can be obtained in accordance to Fig. 5(c). In this figure the dark black continuous waveform represents the flux

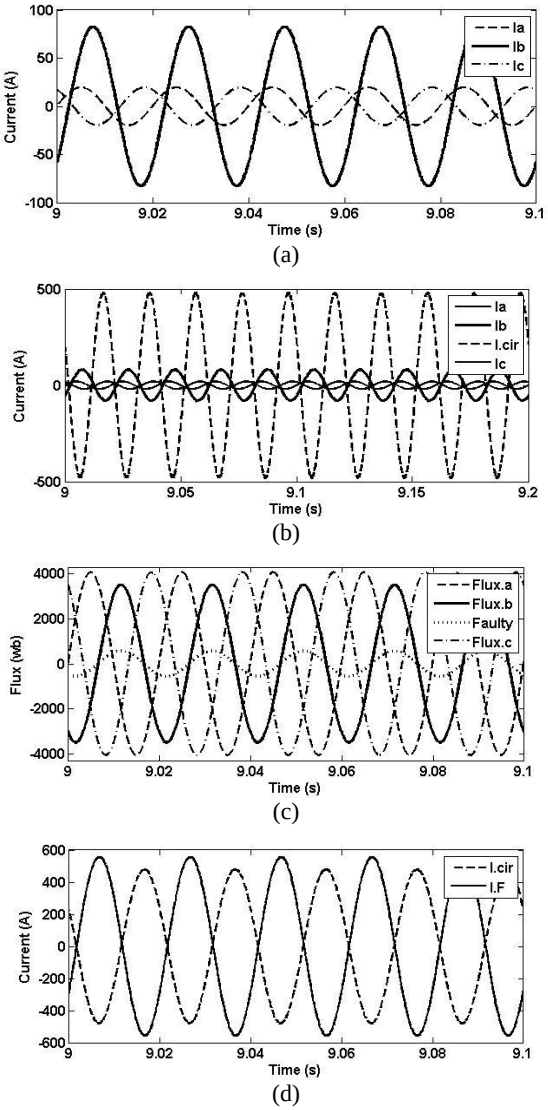

Fig. 5 Waveforms of transformer with inter-turn fault, arising at t=9s by assuming ($N_{sh}=50$ and $R_f=0$). (a) Primary current in three phase. (b) Circulating current along with phase currents. (c) Primary leakage flux along with shunt flux. (d) circulating current along with fault current.

waveform of not shorted segment and the inconspicuous Spotter waveform shows the flux waveform of shorted segment and two other curves represent the flux waveforms of normal phases. Naturally by increasing the shorted turns in the faulty phase, the amplitude of its related waveform will increase. Fig. 5(d), represents the fault current compared with the circulating current. The fault current consists of the circulating current plus the increased current of the faulty winding.

A very important principle in inter-turn fault in transformers is that, the lower, number of shorted turns, the higher is the circulating current and the lower is the primary current. As previously mentioned, the circulating current produces an opposite MMF compared to the fundamental MMF of winding. On the other hand, the supply voltage of the transformer is

assumed to be constant. Subsequently the fundamental MMF of the transformer will not change. Thus, by increasing the shorted turns, the same opposite MMF need to be produced, as it used to. As a result, a lower amount of circulating current is produced. Besides the incremental behavior of circulating current due to decreasing of the shorted turns, also refers to reduction of impedance of the shorted loop. Fig. 6(a) shows the circulating current with the minimum turn ($N_{sh}=1$) which leads to a high amount of current as expected.

Increasing the number of shorted turns will decrease the number of healthy (not shorted) turns and leads to enhancement of primary current. Fig. 6(b) shows the primary current by imposing an inter-turn fault to phase 'B' on primary winding in a three phase transformer, by assuming $N_{sh}=75$ and $R_f=0$, which confirms the incremental behavior of primary current due to increasing the shorted turns of the faulty winding.

The enhancement of primary current caused by increasing the shorted turns, can be seen obviously by comparing Fig. 5(a) and 6(b).

In accordance to Fig. 6(c) and comparing it with Fig. 5(c), the flux enhancement caused by increasing the shorted turns in the faulty winding which is shown by the inconspicuous Spotter waveform can be seen obviously. On the other hand, by increasing the shorted turns in faulty winding, the healthy turns of this winding will decrease. As a result, the flux which is produced by the healthy turns of the faulty winding will decrease as shown by the dark black continuous waveform in Fig. 6(c).

A very significant parameter for controlling the fault and the circulating current is the fault resistance which is naturally caused by insulation defection during the fault occurrence. By increasing the fault resistance, the fault and circulating current will decrease. In other words, the fault severity will decrease. On the other hand by decreasing the fault resistance, the fault and circulating current will increase. In other words, the fault severity will increase. Fig. 7(a) and 7(b) shows different result caused by imposing an inter-turn fault to phase 'B' on primary winding in a three phase transformer, by assuming $N_{sh}=50$ and $R_f=0.25$.

A comparison between Fig. 5(a) and 5(b) and Fig. 7(a) and 7(b) shows that by increasing the fault resistance to 0.25, while we have 50 shorted turns, the primary current will decrease approximately from 80 to 70. On the other hand the circulating current will decrease approximately from 480 to 400 and as a result the fault current will decrease approximately from 560 to 470.

Fig. 7(c) and 7(d) shows different result caused by imposing an inter-turn fault to phase 'B' on primary winding in a three phase transformer, by assuming $N_{sh}=50$ and $R_f=0.5$. In this model we increase the fault resistance from 0.25 to 0.5. Reducing the fault

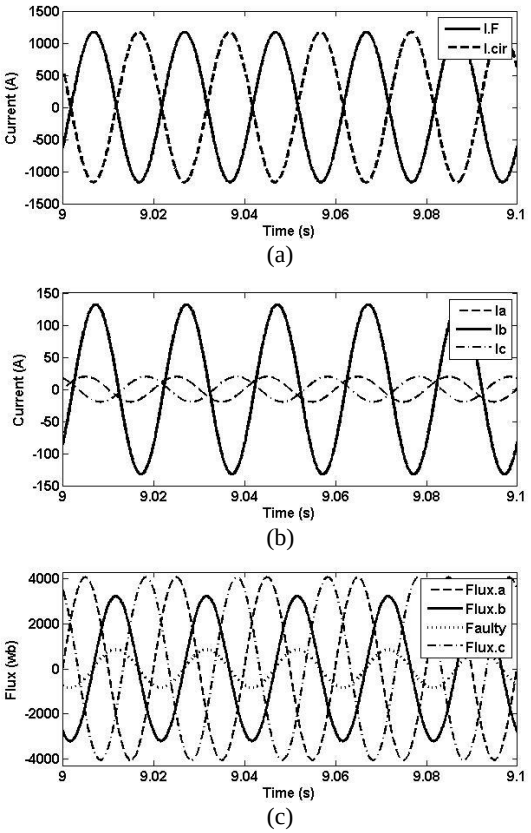

Fig. 6 Waveforms of transformer with inter-turn fault, arising at t=9s by assuming ($N_{sh}=1$ or 75) and ($R_f=0$). (a) Circulating current along with fault current. (b) Primary currents in three phase for ($N_{sh}=75$) and ($R_f=0$). (c) Primary leakage flux along with shunt flux for ($N_{sh}=75$) and ($R_f=0$).

severity after increasing the fault resistance is obvious by comparing Fig. 7(a) and 7(b) with Fig. 7(c) and 7(d).

Fig. 8(a) is a column chart which shows primary currents, considering different fault parameters including variable shorted turns and fault resistances. As already proved, the enhancement of shorted turns in faulty winding will decrease the circulating current which leads to an increment in primary current of the transformer. This figure confirms reducing of fault severity by increasing the fault resistance in accordance to previous simulated figures of our model.

Fig. 8(b) is a column chart which represents the flux in both shorted and healthy turns by changing the number of shorted turns in the faulty winding. This column chart is a brief result from the effect of changing the fault size on flux in the shorted and healthy portion of the faulty winding which is obtained from the simulation of our model and confirms the enhancement of shorted turn flux by increasing the number of shorted turns and consequently decreasing the flux of healthy turns in faulty winding by decreasing the number of healthy turns.

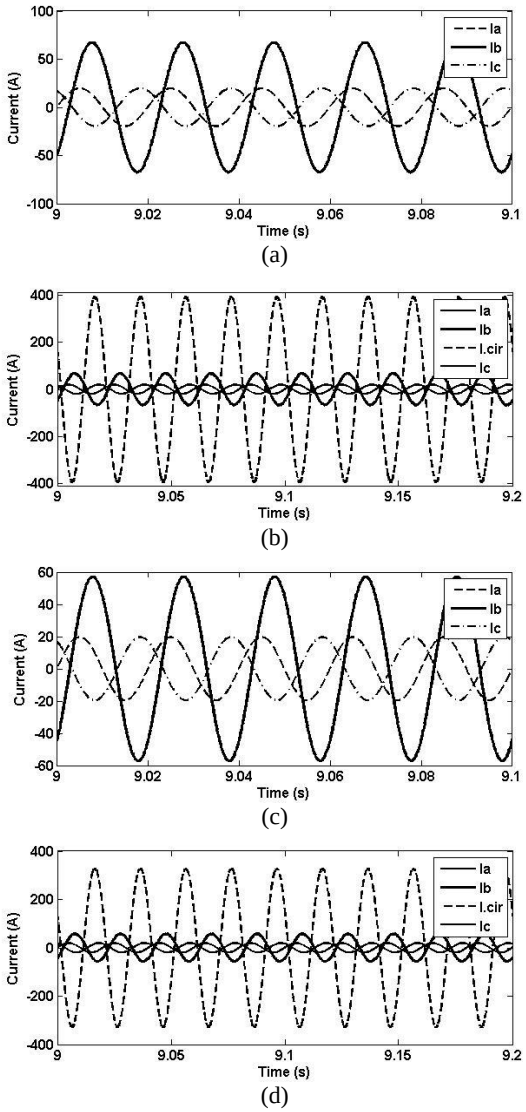

Fig. 7 Waveforms of transformer with inter-turn fault, arising at t=9s by assuming ($N_{sh} = 50$) and ($R_f = 0.25$ or 0.5). (a) Primary currents in three phase for ($N_{sh} = 50$) and ($R_f = 0.25$). (b) Circulating current along with phase current for ($N_{sh} = 50$) and ($R_f = 0.25$). (c) Primary currents in three phase for ($N_{sh} = 50$) and ($R_f = 0.25$). (d) Circulating current along with phase currents for ($N_{sh} = 50$) and ($R_f = 0.25$).

4 Conclusion

This contribution modeled and consequently simulated a distribution transformer, based on mathematical equations both in normal operating condition and also in the presence of an inter-turn fault. The saturation effect is also considered in this model, which is obtained by adding the saturation block to the linear model of the transformer. The mentioned block is an approximation of $\Delta\psi_m$ values, which are written in terms of ψ_m . The model has been used to demonstrate different behaviors of a transformer, considering alterability in the number of shorted turns in the faulty winding and also in fault resistance. The mentioned items are two highlighted distinctions in this study compared other investigations. The results of simulations indicate the remarkable ability of the flexible model to represent the real behavior of a transformer with an inter-turn fault. The mentioned results can be written as follows.

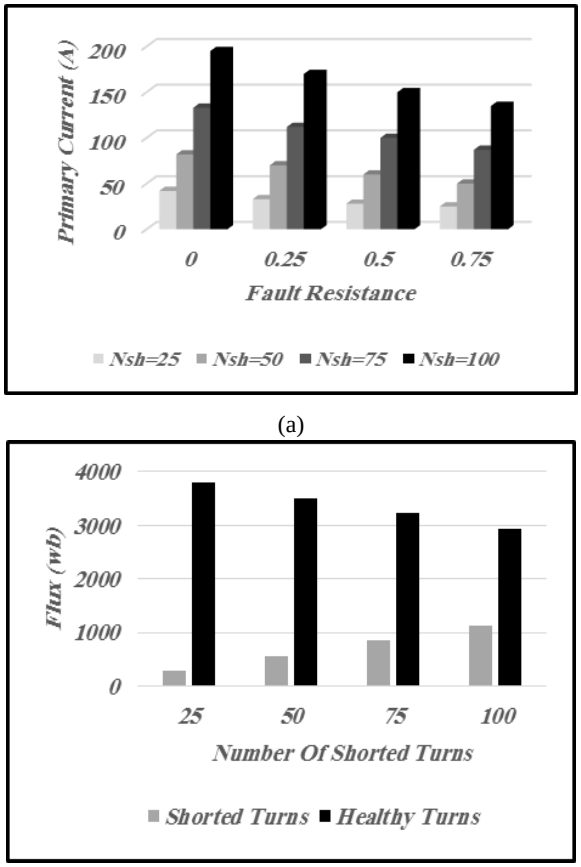

Fig. 8 Primary current and flux measurement. (a) Primary current, considering different fault parameters. (b) Flux in both shorted and healthy turns assuming different shorted turns.

Occurrence of an inter-turn fault, whether in primary or secondary causes a severe circulating current which leads to an increment in the primary current of the faulty phase. It was also found that for the faults on the primary side, the secondary current will remain unaltered. Increasing the number of shorted turns will cause flux enhancement of this segment of the faulty winding. It is noteworthy that, the lower the number of shorted turns, the higher is the circulating current due to reduction of impedance of the shorted loop and the lower is the primary current due to increasing the number of healthy turns in the faulty winding. Thus, an inter-turn fault, including a few turns, has negligible effect on the terminal values of the transformer which

makes the fault detection harder. It was also proved that, by assuming a constant supply voltage, an inter-turn fault will decrease the flux density passing through the core, inside the shorted turns and increases the flux density outside the faulty area. In fact the fundamental linkage flux remains constant. But it mainly passes in redial form around the shorted turns which leads to asymmetrical flux distribution in the transformer. Finally, the last result which is obtained from the simulation is the fault severity which can be controlled by a fault resistance and the number of shorted turns. The minimum fault resistance causes the maximum circulating and primary current. On the other hand, the minimum number of the shorted turns causes the maximum circulating current and minimum increment in primary current.

References

[1] R. S. Bhide, M. S. S. Srinivas, A. Banerjee and R. Somakumar, "Analysis of winding inter-turn fault in transformer: a review and transformer models," *IEEE International Conference on Sustainable Energy Technologies (ICSET)*, pp. 1-7, 6-9 December, Sri Lanka, 2010.

[2] Rajamani.P, Debangshu Dey and Sivaji Chakravorti, "Cross-correlation aided wavelet network for classification of dynamic insulation failure in transformer winding during impulse test", *IEEE Transactions on Dielectrics and Electrical Insulation*, Vol. 18, No. 2, pp. 521-532, April 2011.

[3] Rajamani. P and Sivaji Chakravorti, "Identification of simultaneously occurring dynamic disc-to-disc insulation failures in transformer winding under impulse excitation", *IEEE Transactions on Dielectrics and Electrical Insulation*, Vol. 19, No. 2, pp. 443-453, April 2012.

[4] M. Heidarzadeh and M. R. Besmi, "Influence of the parameters of disk winding on the impulse voltage distribution in power transformers", *Iranian Journal of Electrical & Electronic Engineering (IJEEE)*, Vol. 10, No. 2, pp. 143-151, June 2014.

[5] H. Yaghobi, K. Ansari and H. Rajabi Mashhadi, "Analysis of magnetic flux linkage distribution in salient- pole synchronous generator with different kinds of inter- turn winding faults", *Iranian Journal of Electrical & Electronic Engineering (IJEEE)*, Vol. 7, No. 4, pp. 260-272, Dec. 2011.

[6] J. M. Lunsford and T. J. Tobin, "Detection of and protection for low current winding in overhead distribution transformers", *IEEE Transactions on Power Delivery*, Vol. 12, No. 3, pp. 1241-1249, July 1997.

[7] T. S. Sidhu and M. S. Sachdev, "On-line identification of magnetizing inrush and internal faults in three-phase transformers", *IEEE Transactions on Power Delivery*, Vol. 7, No. 4, pp. 1885-1891, October 1992.

[8] Selwyn Palmer, "Detection of fault in new and old transformers by dissolved-gas analysis", *IET Power Engineering Journal*, Vol. 2, No. 1, pp. 52-54, Jan. 1988.

[9] Joseph J. Kelly, "Transformer fault diagnosis by dissolved-gas analysis", *IEEE Transactions on Industry Applications*, Vol. IA-16, No. 6, pp. 777-782, 1980.

[10] R. R. Rogers, "IEEE and IEC codes to interpret incipient faults in transformers, using gas in oil analysis", *IEEE Transactions on Electrical Insulation*, Vol. EI-13, No. 5, pp. 349-354, October 1978.

[11] ANSI/IEEE Standard C57. 104-1978, IEEE Guide for detection and determination of generated gases in oil-immersed transformers and their relationship to the serviceability of the equipment, pp. 0-1, 1978.

[12] Hadi Afkar and Abolfazl Vahedi, "Detecting and locating tum to tum fault on layer winding of distribution transformer", *5th Conference on Thermal Power Plants (CTPP)*, pp. 109-116, 10-11 June, Iran, 2014.

[13] Paulraj. T, Hari Kishan Surjith. P, Dhana Sekaran. P, "Modeling and location of faults in power transformer using transfer function and frequency response analysis", *IEEE International Conference on Advanced Communications, Control and Computing Technologies (ICACCCT)*, pp. 83-87, 8-10 May, Ramanathapuram, 2014.

[14] A.R. Moniri and S. Farshad, "Modeling the frequency response movements in power transformers for predicting purposes", *Iranian Journal of Electrical & Electronic Engineering (IJEEE)*, Vol. 2, No. 1, pp. 26-33, January 2006.

[15] M. Florkowski and J. Fargul, "A high-frequency method for determining winding faults in transformers and electrical machines", *Review of Scientific Instrument*, Vol. 76, No. 11, pp. 30-38, November 2005.

[16] E. P. Dick and C. C. Erven, "Transformer diagnostic testing by frequency response analysis", *IEEE Transactions on Power Apparatus and Systems*, Vol. PAS97, No. 6, pp. 2144-2153, November 1978.

[17] J. Pleite, C. Gonzalez, J. Vazquez, and A. Lazaro, "Power transformer core fault diagnosis using frequency response analysis", *IEEE Mediterranean Electrotechnical Conference*, pp. 1126-1129, 16-19 May, Spain, 2006.

[18] Ch. P. Babu1, M. Surya kalavathi, and B.P.Singh, "Use of wavelet and neural network (BPFN) for transformer fault diagnosis", *IEEE Conference on Electrical Insulation and Dielectric Phenomena*, pp. 93-96, 15-18 October, Kansas City, 2006.

[19] E.A. Mohamed, A.Y. Abdelaziz and A.S. Mostafa, "A neural network-based scheme for fault diagnosis

of power transformers", *Electric Power Systems Research*, Vol. 75, No. 1, pp. 29–39, July 2005.
[20] P. Arboleya, G. Diaz, C. Gonzailez-Morain, and J. G-Aleixandre, "A wavelet approach applied to transformer fault protection: signal processing", *The International Conference on Computer as a Tool (EUROCON)*, pp. 1634-1637, 21-24 November, Belgrade, 2005.
[21] K. Ramesh and M.Sushama, "Inter-Turn fault detection in power transformer using fuzzy logic", *International Conference on Science Engineering and Management Research (ICSEMR)*, pp. 1-5, 27-29 Novemver, Chennai, 2014.
[22] V. Behjat, A. Vahedi, "Numerical modelling of transformers inter-turn fault and characterising the faulty transformer behavior under various faults and operating conditions", *IET Electric Power Applications*, Vol. 5, No. 5, pp. 415–431, May 2011.
[23] Shantanav Bhowmick and Subhasis Nandi, "Online detection of an inter-turn winding fault in single-phase distribution transformers using a terminal measurement-based modeling technique", *IEEE Transactions on Power Delivery*, Vol. 30, No. 2, pp. 1007-1015, April 2015.
[24] Gusman Diaz Gonzalez, Javier Gumez, Aleixandre Fernandez and Pablo Arboleya, "Electromagnetic model of turn-to-turn short circuits in transformers", *The International Journal for Computation and Mathematics in Electrical and Electronic Engineering*, Vol. 23, No. 2, pp. 558-571, 2004.
[25] Luıs M. R. Oliveira and Antonio J. Marques Cardoso, "Leakage inductances calculation for power transformers inter-turn fault studies", *IEEE Transactions on Power Delivery*, Vol. 30, No. 3, pp. 1213-1220, June 2015.
[26] R S Bhide, Srinivas M. S. S., and Ilia Voloh, "Detection of inter-turn fault in transformers at incipient level", *International Conference on Electrical Machines (ICEM)*, pp. 1542-1548, 2-5 September, 2014.
[27] P. Bastard et al., "A transformer model for winding fault studies", *IEEE Transactions on Power Delivery*, Vol. 9, No. 2, pp. 690 - 699, April 1994.
[28] Luís. M. R. Oliveira and A. J. Marques Cardoso, "A permeance-based transformer model and its application to winding interturn arcing fault studies", *IEEE Transactions on Power Delivery*, Vol. 25, No. 3, pp. 1589 - 1598, July 2010.
[29] Chee-Mun Ong, *Dynamic simulation of electric machinery using matlab / simulink*, Chapter 3 and 4, A Simon & Schuster Company, Upper saddle river, New Jersey, USA: Prentice-Hall, 1998.

Mehdi Samami was born in Nowshahr, Iran, in 1984. He received his B.S degree in electrical engineering from South Tehran Branch, Islamic Azad University, Tehran, Iran, in 2007. He Graduated in M.S degree in the department of Electrical Engineering, Mazandaran Science and Research Branch, Islamic Azad University, Sari, Iran in 2015. He is currently a Ph.D. student in the department of Electrical Engineering, Sari Branch, Islamic Azad University, Sari, Iran. Since 2009 up to now, he has been with the Mah Taab Caspian Electricity Generation Company, Technical Bureau of Nowshahr Power Plant in Iran. His research interests include analysis, design and protection of electrical machines.

Hamid Yaghobi was born in Sari, Iran on 1978. He received his B.Sc. degree in Electrical Engineering from K.N.Toosi University of Technology in 2000, Tehran, Iran, M.Sc degree in Electrical Engineering from Ferdowsi University in 2002, Mashhad, Iran and his Ph.D. in electric machinery from the Department of Electrical Engineering of Ferdowsi University, Mashhad, Iran in 2011. He is currently an Assistant Professor at Semnan University. His research interests are modeling and fault diagnosis, design and protection of electrical machines.

Milad Niaz Azari was born in Babol, Iran, in 1984. He received his B.S degree in electrical engineering from Noshirvani University of Technology, Babol, Iran in 2007. He Graduated in M.S degree in the department of Electrical Engineering, Amir Kabir University of Technology, Tehran, Iran in 2009. Also he graduated in Ph.D. degree in Amirkabir University of Technology, Tehran, Iran in 2013. Since 2014, he has been at University of Science and Technology of Mazandaran , Behshahr, Iran, as an assistant Professor in the department of Electrical Engineering. His areas of interest are electrical machines design and power electronics.